Developmental Biology **242,** 44–57 (2002)
doi:10.1006/dbio.2001.0516, available online at http://www.idealibrary.com on IDEAL®

Genetic Mosaic Analysis Indicates That the Bulb Region of Coat Hair Follicles Contains a Resident Population of Several Active Multipotent Epithelial Lineage Progenitors

Raphael Kopan,*,[1] Jonghyeob Lee,* Meei-Hua Lin,* Andrew J. Syder,* John Kesterson,† Neil Crutchfield,* Caroline R. Li,* Wei Wu,* Jason Books,* and Jeffrey I. Gordon*

**Department of Molecular Biology and Pharmacology, Washington University School of Medicine, St. Louis, Missouri 63110; and †VayTek, Inc., Fairfield, Iowa 52556*

The hair follicle represents an excellent model system for exploring the properties of lineage-forming units in a dynamic epithelium containing multiple cell types. During its growth (anagen) phase, the proximal–distal axis of the mouse coat hair (pelage) follicle provides a historical record of all epithelial lineages generated from its resident stem cell population. An unresolved question in the field is whether the bulb region of anagen pelage follicles contains multipotential progenitors and whether their individual contribution to cellular census fluctuates over time. To address this issue, chimeric follicles were harvested in midanagen from three types of genetic mosaic mouse models. Analysis of the distribution of genotypic markers, including digital three-dimensional reconstruction of serially sectioned chimeric follicles, revealed that on average the bulb contains four or fewer active progenitors, each capable of giving rise to all six follicular epithelial fates. Moreover, analysis of mosaic pelage, as well as cultured whisker follicles provided evidence that bulb-associated progenitors can give rise to expanding descendant clones during midanagen, leading to the conclusion that the bulb contains dormant or symmetrically dividing stem cells. This latter feature resembles the behavior of hematopoietic stem cells after bone marrow transplantation, and raises the question of whether this property may be shared by stem cells in other self-renewing epithelia.

Key Words: **stem cells; hair follicle; epithelial differentiation; genetic mosaic mouse models.**

INTRODUCTION

The hair follicle is a distinctive stratified epithelium that renews itself in anatomically distinct compartments, has well-defined patterns of cellular organization, and periodically undergoes cycles of destruction and reconstruction. Each follicle, irrespective of its location in the body, has radial symmetry about its proximal-to-distal axis, and is asymmetric along its proximal-to-distal axis. At its proximal end, the follicle contains an epithelium that surrounds a teardrop-shaped dermal papilla composed of mesodermal cells in the trunk and ectomesoderm in the head (Fig. 1A). Cells in the dermal papilla are the source of inductive signals required for growth and differentiation of the epithelium (Hardy, 1992; Kishimoto *et al.*, 2000; Sengel, 1976).

The bulb is the portion of the follicle that contains the dermal papilla and its associated epithelium. The base of the bulb is populated by poorly differentiated epithelial cells (Coulombe *et al.*, 1989; Reynolds and Jahoda, 1991). These cells, together with a population of TA keratin-positive cells, form the matrix. Cells distal to the matrix have withdrawn from the cell cycle and are in the process of terminal differentiation into six distinct cell types (Fig. 1A). Differentiating postmitotic members of each epithelial lineage form a homogenous cellular cohort that encircles the follicle, creating concentric, cell type-specific arrays that surround the anterior–posterior axis of the follicle (Fig. 1A). These cellular cohorts move upward.

The coat hair (pelage) follicle undergoes periods of de-

[1] To whom correspondence should be addressed. Fax: (314) 362-7058. E-mail: kopan@molecool.wustl.edu.

0012-1606/02 $35.00

struction followed by reconstruction. Each hair cycle begins with a growth phase (anagen) where the structures shown in Fig. 1A are continuously generated. This growth phase is curtailed by a destructive phase (catagen) that removes all proliferating undifferentiated cells from the bulb, leaving the upper third of the follicle and dermal papilla intact during the resulting rest phase (telogen). Subsequent entry into anagen is believed to begin when signals from a dermal papilla activate stem cells in the bulge (Stenn and Paus, 2001). Mechanical or chemical removal of pelage follicles at any phase of the growth cycle leads to induction of another anagen. Studies suggest that, if mechanical/chemical removal occurs during anagen, the initiation of a new cycle involves activation of residual *bulb*-associated germinative cells (Hale and Ebling, 1975; Johnson and Ebling, 1964).

There has been considerable debate over the years about whether the bulb of anagen pelage follicles contains active multipotent stem cells (Cotsarelis *et al.*, 1999; Coulombe *et al.*, 1989; DasGupta and Fuchs, 1999; Fuchs *et al.*, 2001; Huelsken *et al.*, 2001; Merrill *et al.*, 2001; Reynolds and Jahoda, 1991, 1996; Rochat *et al.*, 1994; Tani *et al.*, 2000). Several models can be envisioned to explain the origin and placement of the various epithelial lineages that comprise the pelage follicle (Fig. 1B). One model has the active multipotent stem cell limited to the *bulge*. The descendants of this cell become restricted to a single fate based on instructions they receive from the dermal papilla: such instructions could either be received during bulge "activation" (Taylor *et al.*, 2000) or when migrating bulge cells enter the bulb (Oshima *et al.*, 2001). These unipotential cells, and/or their daughters, then stream upwards in cohorts from the bulb to define the lamellar structure of the epithelium (model 1 in Fig. 1B). Another view (model 2 in Fig. 1B) is that the matrix contains bulge-derived oligopotential progenitors that can give rise to more than one, but not all, cell types. The dermal papilla contributes to defining their lineage restriction. During a subsequent upward migration, descendants of these cells become restricted to a single fate, either through cell autonomous or nonautonomous mechanisms. The timing and location of this lineage restriction defines the lamellar structure of the follicle. The third model shown in Fig. 1B invokes a matrix-associated progenitor whose potential is equivalent to that of the multipotent bulge stem cell. (Note the term "multipotent" is only being used here with regard to follicular epithelial cell fates; the potential to give rise to epidermal and sebaceous gland cell lineages is not being considered; Fuchs *et al.*, 2001; Taylor *et al.*, 2000.) This postulated multipotent *bulb* progenitor would give rise to descendents whose commitment to a particular fate is defined by their position relative to the dermal papilla (organizer) and/or through cell–cell interactions. In model 3, the lamellar structure of the follicular epithelium would reflect the positional threshold values of the organizing signal(s).

Retroviral tagging experiments using reconstituted skin have provided evidence for the oligo-lineage progenitors invoked in model 2 (Kamimura *et al.*, 1997). Follicular skin was reconstituted by mixing primary keratinocytes, 10–20% of which are infected with a helper-free retrovirus expressing human alkaline phosphatase (AP), with dermal papilla cells. The mixture was introduced into a transplantation chamber, which was implanted in nude mouse recipients. The resulting hair follicles were analyzed 6 weeks later (presumably in third anagen). Follicles generated following these experimental manipulations contained several progenitors that gave rise to AP-positive descendants. These descendants were typically organized into concentric rings of wholly AP-positive cells, leading to the conclusion that the bulb is populated by partially committed (oligo-potential) progenitors.

Intriguingly, this reconstitution paradigm has also provided support for model 3. Topley *et al.* (1999) found that, if $p21^{-/-}$ keratinocytes were used, the resulting follicles typically were uniformly AP-positive (i.e., monoclonal). Such a finding indicates the existence of retrovirus-infectable multipotent progenitors (Topley *et al.*, 1999). However, since chimeric mouse studies have definitively established that pelage follicles are normally polyclonal (Mintz and Bradl, 1991; Mintz and Silvers, 1970), monoclonal AP-positive follicles could reflect an increased proliferative activity of p21-deficient multipotent stem cells which could make them more amenable to infection.

Retroviral experiments that used an injury (derm-abrasion) rather than a reconstitution model have also produced results that do not permit model 2 or 3 to be eliminated. For example, Ghazizadeh and Taichman (2001) examined follicles formed after derm-abrasion and subsequently maintained *in situ* for >36 weeks through five or six cycles of depilation-induced hair loss and regeneration. Lineage-restricted distribution of a retroviral-encoded LacZ tag was observed, as predicted by model 2. However, uniformly labeled follicles were also detected.

A remarkable observation made during these latter long-term studies is that 45% of follicles either had a labeled bulb (43%), or labeled bulge (2%), but not both (Ghazizadeh and Taichman, 2001). This demonstrates that the bulb is maintained by a stem cell population that can survive multiple depilation-induced hair cycles (Ghazizadeh and Taichman, 2001) and that these progenitors are not in the bulge. It also suggests that the self-renewing potential of bulb progenitors can far exceed the length of one hair cycle—a feature not normally detectable since they are normally executed at the end of anagen (Stenn and Paus, 2001).

Taken together, these retroviral studies of injured or reconstituted mouse skin reveal at a minimum that the bulb contains long-lived, oligo-potential progenitors. In this paper, we have used chimeric mice, generated using three different methods, to provide evidence in support of model 3 where the bulb contains a resident population of four or fewer active multipotent progenitors. Moreover, our findings suggest that the ability of some multipotent stem cells to generate descendant clones varies during the course of anagen.

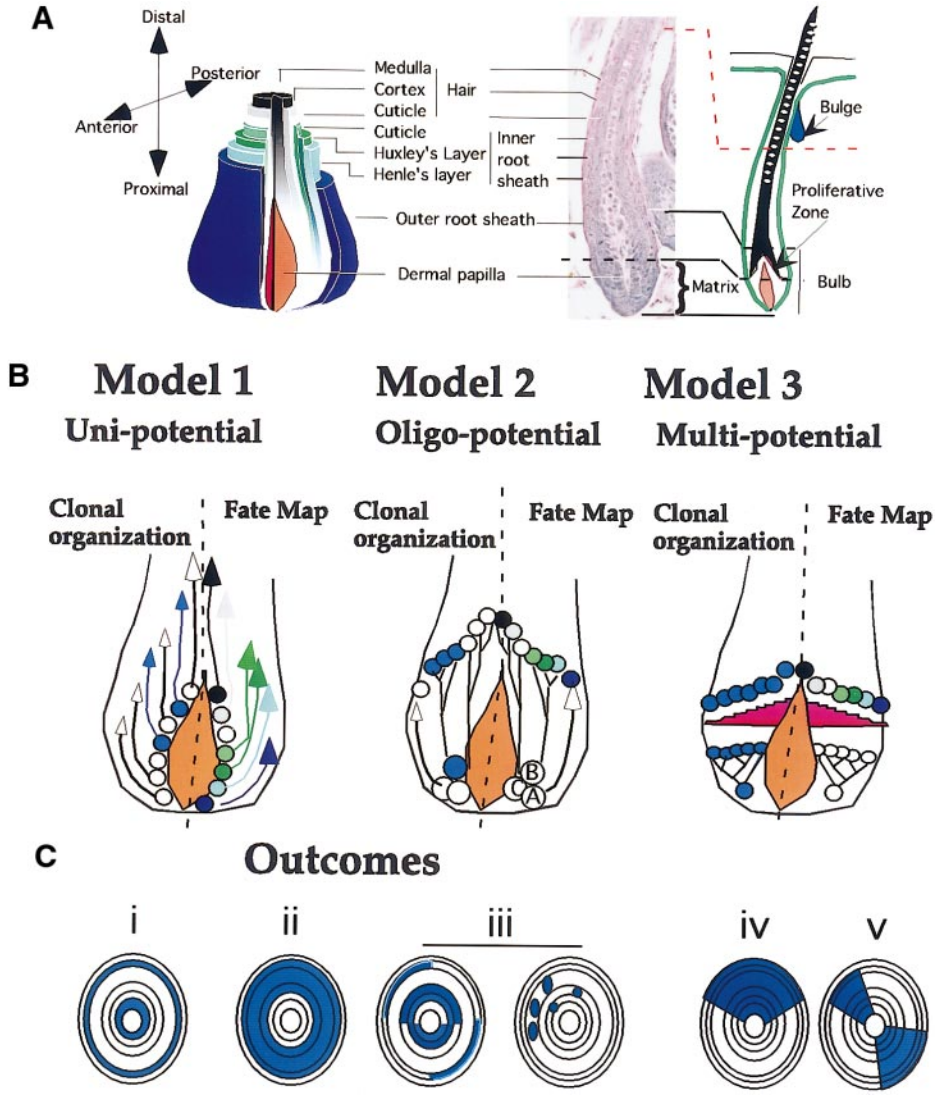

FIG. 1. Possible models of the stem cell hierarchy in chimeric anagen follicles. (A) Follicular architecture. (Left) A schematic overview of the organizational features and cellular composition of the bulb region. Transiently amplifying cells in the matrix give rise to six different cell types that form concentric rings along the anterior–posterior (A-P) axis of the follicle. An innermost column of epithelial cells extends from the tip of the dermal papilla (DP) and forms the medulla. Two rings of cells surround the medulla: the cortex and cuticle. The medulla, cortex, and cuticle constitute the hair shaft. The hair shaft is surrounded by three rings of cells that form the inner root sheath (IRS): the IRS cuticle, Huxley's layer, and Henle's layer. Cells that form the outer root sheath (ORS) surround the IRS and extend from the base of the follicle upwards until they blend with cells in the basal layer of the epidermis. (Middle) Hematoxylin and eosin-stained section of the lower half of an anagen pelage follicle. (Right) Schematic overview of the intact pelage follicle. (B) Three possible models of clonal organization in the bulb. Each panel is subdivided into two halves. The left half outlines a clonal organization (blue = LacZ+ $B6^{ROSA26+/-}$ lineage progenitors). The right half is a mirror image of the left displaying cell fate choices (color of descendant lineages follows the scheme used in A). See text for further discussion. (C) Model-based outcomes anticipated from an analysis of chimeric follicles sectioned perpendicular to the P-D axis. Outcomes i–iii are possible with models 1 and 2 and reflect differences in the number of active stem cells. Outcomes iv and v would only be anticipated from model 3 and differ from one another based on the number of active progenitors.

MATERIALS AND METHODS

Generation of chimeric mice. Chimeric mice were produced either by injecting D3 129/Sv embryonic stem (ES) cells into C57/Bl/6 $(B6)^{ROSA26/+}$ blastocysts (Wong *et al.*, 1998) or by aggregating $CD1/B6^{+/+}$ morulae with $CD1/B6^{ROSA26/+}$ morulae (Hogan, 1994). In addition, female TgN(GFPX)4Nagy mice (The Jackson Laboratory) containing chicken β-actin-GFP transgene integrated on the X-chromosome were studied. All mice were maintained in specified pathogen-free state, in a barrier facility, and given free

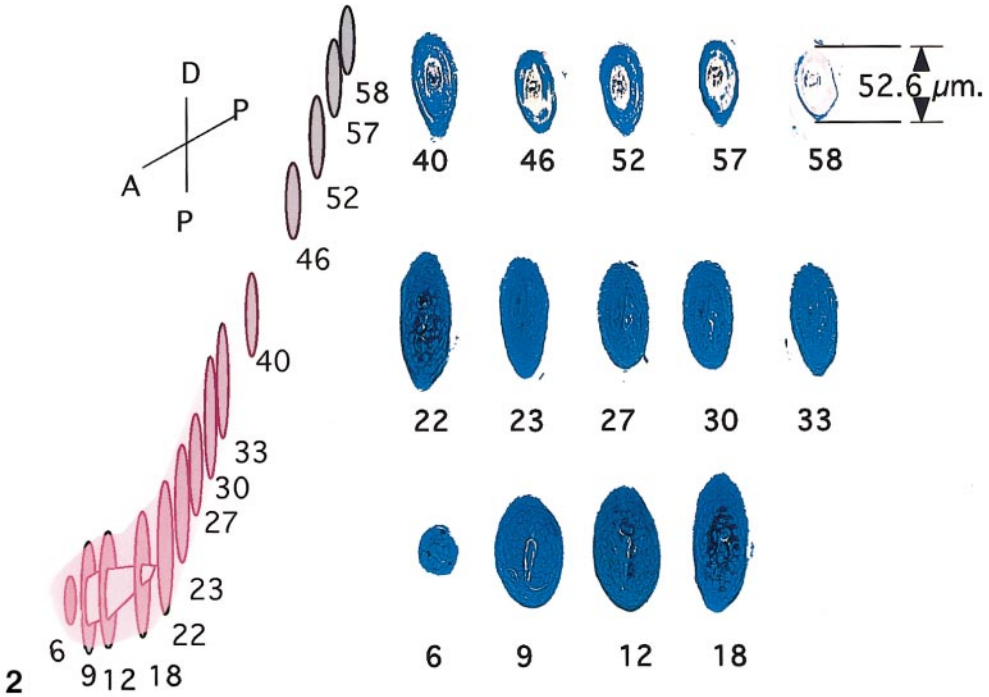

2

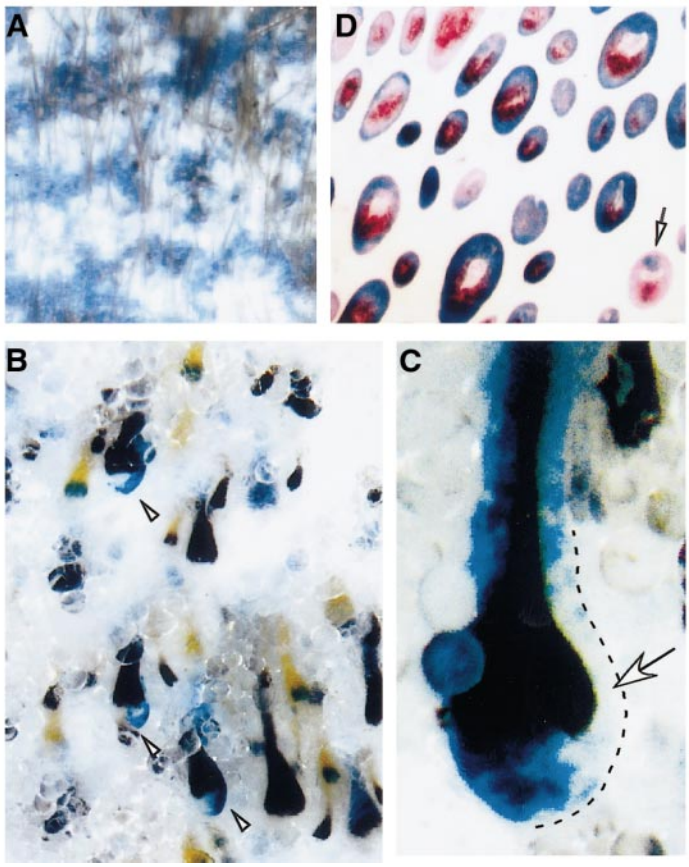

3

access to a standard irradiated chow diet (PicoLab Rodent Chow 20; Purina Mills Inc.).

Histochemical studies. Adult chimeras (8–12 weeks old) were subjected to depilation as follows. Following general anesthesia, the dorsal hair was clipped, and hair stubs were removed with either wax strips, or a commercially available preparation of calcium hydroxide (Nair; Carter-Wallace, New York). Animals were monitored daily until hair follicles erupted above the skin surface (7–10 days after depilation). Mice were then sacrificed, a $4 \times 6\text{-cm}^2$ region of anagen growth was removed, and the tissue was placed in phosphate-buffered saline (PBS) and pinned out on a wax sheet (dermis side up). The underlying muscle and adipose tissues were dissected away, and the skin was subsequently fixed in periodate–lysine–paraformaldehyde (30 min, 23°C). Following three washes in PBS, the tissue was placed in a solution of PBS containing 2 mM 5-bromo-4-chloro-3-indolyl β-D-galactosidase (X-Gal), 2 mM $MgCl_2$, 4 mM potassium ferricyanide, 4 mM potassium ferrocyanide, 0.01% sodium deoxycholate, and 0.02% IGEPAL CA-630 (Sigma), and incubated at 4°C for 36 h in the dark. Whole-mount preparations of fixed, X-Gal-stained skin were screened under a dissecting microscope to identify and photograph regions containing chimeric follicles. These regions were recovered and embedded in paraffin, and serial 5-μm sections were prepared, either parallel or perpendicular to the anterior–posterior axis of the hairs. Some sections were counterstained with nuclear fast red.

Analysis of skin from 11-day-old TgN(GFPX)4Nagy mice was performed as above with the following modifications. After fixation in PLP, the skin was incubated in 20% sucrose/PBS (24 h, 4°C). Frozen sections were counterstained with propidium iodide and photographed. The GFP expression pattern was independently confirmed by immunohistochemistry (see below).

Immunohistochemistry. Deparaffinized sections of skin were rehydrated, incubated in 10 mM sodium citrate (pH 6.0; 45 min, 100°C in a rice cooker), and then allowed to cool (30 min, 23°C). After two PBS washes (5 min each), slides were incubated in blocking buffer (1.2% normal horse serum in PBS). Anti-Tcf-3/4 (mouse monoclonal clone 6F12–3, Upstate Biotechnology, 1:1000 dilution in blocking solution) was placed on the slides and incubated overnight at 4°C. After a second round of PBS washes, slides were incubated with biotinylated horse anti-mouse Ig (Vector Laboratories; 1:2000). Antigen–antibody complexes were visualized by using ABC reagent (Vector Laboratories), followed by amplification with biotin-tyramide (NEN Life Science; diluted 1:50 in Amplification Diluent), and staining with Texas Red Avidin D (Fluorescent Avidin Kit; Vector Laboratories).

Dorsal skin was removed from 11-day-old TgN(GFPX)4Nagy mice, fixed with 2% paraformaldehyde in PBS (30 min, 23°C), saturated with 10 and 30% sucrose in PBS overnight, embedded in OCT, and quickly frozen, and 7-μm-thick sections were prepared. Sections were then thawed and washed in PBS, and endogenous peroxidase activity was blocked (0.3% hydrogen peroxidase in PBS). Following washes in PBS and treatment with blocking buffer, rabbit anti-GFP (Chemicon; 1:100) was added. After a second round of PBS washes, slides were incubated with biotinylated goat anti-rabbit Ig (Vector Laboratories, 1:500). Antigen–antibody complexes were visualized by using ABC reagent (Vector Laboratories) followed by DAB substrate (Immuno-Pure Metal Enhanced DAB Substrate Kit; Pierce).

Culturing whisker follicles. Protocols were adopted from a previous report (Philpott *et al.*, 1996) with the following modifications. Whiskers pads were removed from 10-day-old TgN(GFPX)4Nagy pups immediately after sacrifice. Individual whisker follicles were separated from their capsule (Oliver, 1966) and washed in Williams E medium, and the hair was inserted into a strip of silicone grease located in a plate containing Williams E medium, supplemented with L-glutamine (2 mM), insulin (10 ng/ml), hydrocortisone (10 ng/ml), and penicillin/streptomycin (100 U/ml). This allowed the whisker to be immobilized and photographed at various times from the same vantage point (see below). The dermal papilla was removed from a few whiskers to provide nongrowing controls.

Digital photography and 3-D reconstruction of chimeric follicles. Images were collected from comparable regions of 150 adjacent serial sections per skin sample, using a Quantex Digital Camera (Photometrics). Each region of each section was photographed three times by using color separation filters. Eight-bit images were then merged (Image-Pro Plus software; Media Cybernetics, Silver Spring, MD) to generate 24-bit RGB color images. RGB images from 24–50 serial sections were used for each three-dimensional (3-D) reconstruction. To do so, images were first aligned by using a software package written for this study and now available from VayTek (http://www.vaytek.com). Aligned images (x- and y-axes) were stacked, together with blank images, to reconstruct the z-axis using utilities incorporated into the software package. The stacks were imported into the volume rendering program, VoxBlast (http://www.vaytek.com/VoxBlast.html), which generates 3-D projections from the registered 2-D images. The 3-D projections were viewed by using alpha blending or surface rendering algorithms, converted into QuickTime movies (http://www.apple.com/quicktime/), and formatted for viewing on a website (http://molecool.wustl.edu/kopan.movies.html).

Individual, cultured, and immobilized GFP chimeric follicles were photographed daily (Zeiss AxioCam camera) through a UV lamp- and GFP filter-equipped Olympus SZH12 stereoscope. Images were acquired by using Zeiss AxioVision (v3.0) software. GIF images were looped into a movie by using GFBuilder Software.

FIG. 2. Serial sections of an anagen follicle from an adult C57/Bl/$6^{ROSA\text{-}26+/-}$ mouse. Serial sections (5 μm) were prepared from X-Gal-stained whole mounts of dorsal skin. A schematic of the orientation and number of each section is provided on the left. Each section was counterstained with nuclear fast red. The bulb (sections 6–23) consists of a wholly LacZ+ population of blue cells. LacZ activity is lost in distal, fully keratinized dead cells (sections 40 and higher).

FIG. 3. X-Gal-stained whole-mount preparation of dorsal skin from an adult $129/Sv^{+/+} \leftrightarrow B6^{ROSA26/+}$ chimeric mouse. (A) Low magnification view of dorsal skin. (B) Ventral view of dorsal skin from a mouse sacrificed 10 days after depilation, showing several chimeric follicles (e.g., arrowheads) composed of mixtures of blue and white epithelium surrounding hairshafts. 129/Sv cells contain the *agouti* allele, and hence metabolize melanin to red–yellow phaeomelanin, forming a brown pigment in the hair shaft. B6 cells are able to metabolize melanin to the brown–black eumelanin, and hence appear black. (C) High-power view of a chimeric follicle composed of 129/Sv and $B6^{ROSA26/+}$ epithelial cells. The arrow points to the 129/Sv LacZ− cellular cohort. (D) Section containing a cluster of chimeric follicles. The open arrow points to one of several follicles in the field with sectors, as predicted by model 3 (outcome "v" in Fig. 1C). This follicle has four clearly demarcated sectors, each with a LacZ phenotype opposite to that of its immediate neighbor (see Fig. 5B for a 3-D reconstruction).

RESULTS AND DISCUSSION

Chimeric mice were produced by injecting 129/Sv ES cells into C57/Bl/6 (B6) blastocysts heterozygous for the ROSA26 locus (Zambrowicz *et al.*, 1997). $B6^{ROSA26/+}$ mice express *Escherichia coli* β-galactosidase (LacZ) in virtually all cell lineages during the course of their development and through adulthood. Figure 2 shows an anagen-stage follicle from a young adult $B6^{ROSA26/+}$ mouse stained with X-Gal, counter-stained with nuclear fast red, and then sectioned along its proximal–distal axis. LacZ is expressed in all epithelial and mesenchymal cells in the bulb (e.g., sections 9 and 12 in Fig. 2). All members of each epithelial cell lineage are LacZ+ as they move through the lower third of the follicle (sections 6–33 in Fig. 2). It is only after these cells senesce and undergo complete keratinization (as members of the hair shaft and the upper limits of the inner root sheath) that they lose their ability to express the ROSA26-LacZ reporter (sections 46–58 in Fig. 2). Therefore, we confined our analysis of hair follicles in $129/Sv^{+/+} \leftrightarrow B6^{ROSA26/+}$ chimeras to the lower half of anagen-stage follicles. To synchronize anagen follicles, 8- to 12-week-old chimeras were depilated and sacrificed ~2 weeks later as new hairs emerged on their backs.

Predicted Patterns of Chimerism in Anagen Pelage Follicles Recovered from $129/Sv^{+/+} \leftrightarrow B6^{ROSA26/+}$ Mice

Figure 1C shows the patterns of chimerism that would be predicted from the three models presented in the Introduction. We have assumed that, in chimeric hair follicles, as in other chimeric tissues, cells of each genotype are able to mix randomly and thoroughly with one another (Gardner and Cockroft, 1998). Model 1 has each of the six epithelial lineages derived from one or more active unipotential progenitor(s). Therefore, members of all lineages could be either B6 (LacZ+) or 129/Sv (LacZ−). The number of active progenitors in the bulb would determine the size of the lineage cohort/genotype. If all members of a particular lineage are derived from a single active progenitor, then a discrete ring of cells of a single genotype should be encountered in chimeric pelage follicles at some frequency (outcome "i" in Fig. 1C). If members of one lineage are generated from several active unipotential progenitors, the ring should be composed of a mixture of alternating clusters of cells of each genotype along the anterior–posterior axis (outcomes "ii" or "iii" depending on the number of progenitors that reside in a bulb).

Model 2 postulates an oligo-potential lineage progenitor capable of giving rise to more than one, but not all, epithelial cell types (e.g., the blue oligo-lineage progenitor in Fig. 1C gives rise to all cell types of the inner root sheath). Depending on the number of active oligo-lineage progenitors per fate, the patterns of chimerism would be similar to those postulated for model 1, except that if there is a single active oligo-lineage progenitor its descendants could contribute to multiple adjacent rings of a given genotype (outcome "ii" in Fig. 1C). Outcomes i–iii are all possible: the frequency of each outcome would depend on the number of progenitors that populate each follicle.

Model 3 proposes multipotent bulb progenitors capable of contributing descendants to all cell types (layers) along the anterior–posterior axis of the hair follicle. It can be distinguished from the other two models because it predicts that the descendants of this multipotent progenitor will be organized in sectors, rather than rings, composed of either LacZ+ (blue) $B6^{ROSA26/+}$ or LacZ− (white) 129/Sv cells. The number of sectors will reflect the number of active progenitors (compare outcomes iv and v with outcomes i–iii in Fig. 1C).

The Pattern of Chimerism Observed in Pelage Follicles of $129/Sv^{+/+} \leftrightarrow B6^{ROSA26/+}$ Chimeras Provides Evidence for the Existence of Active Multipotent Stem Cells in the Bulb

X-Gal was used to stain whole-mount preparations of adult $129/Sv^{+/+} \leftrightarrow B6^{ROSA26/+}$ skin harvested during synchro-

FIG. 4. Serial sections of two anagen follicles with sectors. (A) Four serial sections of two adjacent follicles (chimeric on left, $B6^{ROSA-26/+}$ alone on right). Each follicle has been sectioned along its proximal–distal axis. (B) Representative serial sections of a chimeric follicle sectioned obliquely to the P-D axis (orientations of sections are shown in the schematic diagram on the left). Clusters of LacZ+ or LacZ− cells have a single X-Gal staining pattern: e.g., see the monophenotypic columns of cells on either side of the axis of symmetry denoted by the dashed line placed in one the sections shown in (A), or the monophenotypic sectors visible in sections 22 and 23 of (B). (C) A Tcf-3/4-positive population of cells located at the base of the bulb.

FIG. 5. Three-dimensional reconstruction of the bulbs of chimeric anagen pelage follicles from $129SV^{+/+} \leftrightarrow B6^{ROSA26/+}$ mice reveals two types of clonal organization. (A, B) The majority of clones in chimeric follicles consist of coherent groups of cells that extend along the P-D axis. The left panels in (A) and (B) show single, hematoxylin and eosin-stained, obliquely cut sections from two different serially sectioned chimeric follicles. The middle panels show the same sections but with arbitrarily assigned colors (to enhance contrast for subsequent 3-D reconstructions). The right panels are stereo-views of single frames from a movie showing a 3-D reconstruction generated by using all of the serial sections from each follicle (see movie A at http://molecool.wustl.edu/kopan.movies.html). In (B), the red color has been removed, so that only the descendants of the "blue" clone are shown together with cells from the dermal papilla (green) (see movie B at http://molecool.wustl.edu/kopan.movies.html). (C) A chimeric follicle showing a clone (pink–red) that does not extend along the length of the P-D axis but rather is cloistered in the bulb (see movies C and D at http://molecool.wustl.edu/kopan.movies.html; note that melanin granules in movie D are colored green, as in the middle panel of panel C, to provide a landmark for the 3-D reconstruction).

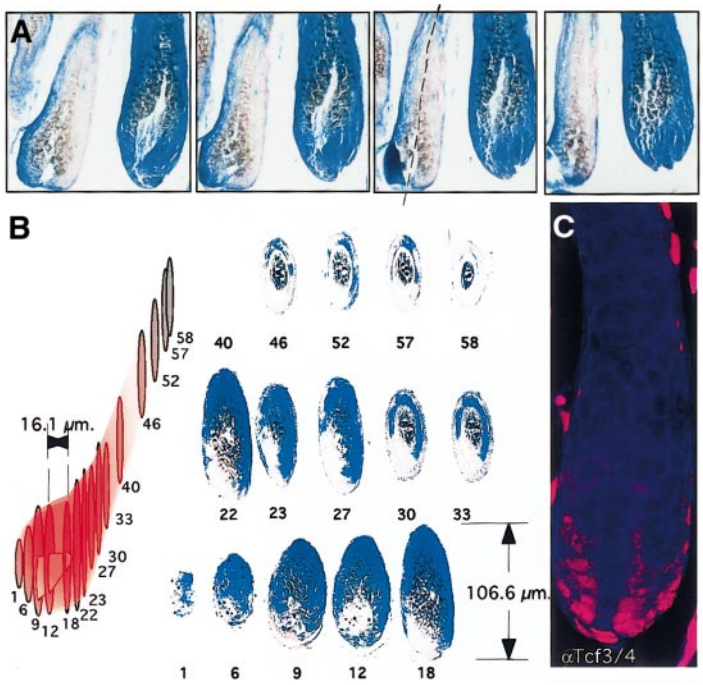

4

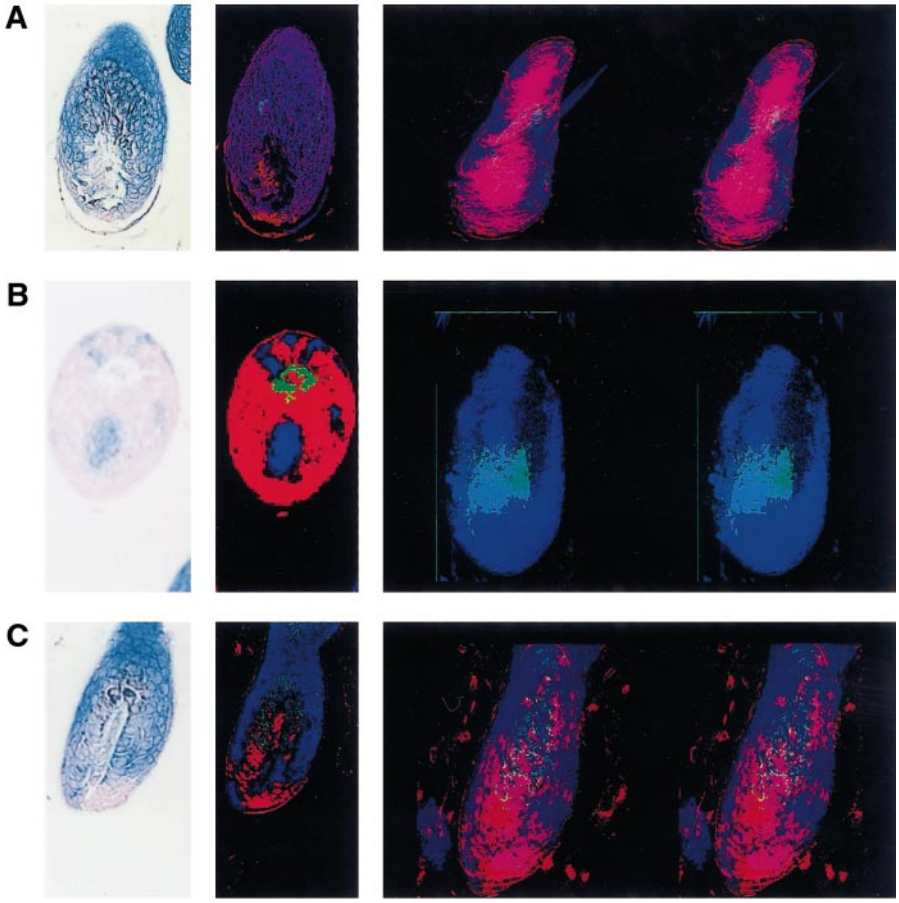

5

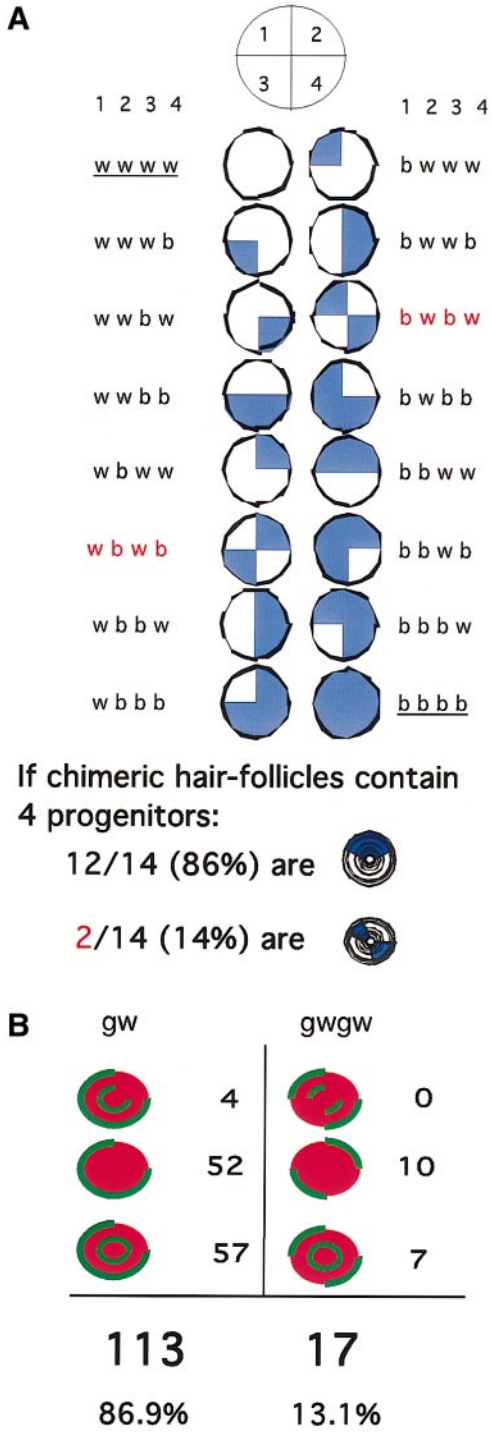

FIG. 6. Predicted and observed patterns of genetically marked clones in chimeric anagen pelage follicles. (A) In the hypothetical follicle, four sectors (numbered 1–4) can contain cells expressing LacZ (blue, b) or cells that are LacZ− (w, white). All the possibilities in $(w + b)^4 = w^4 + \mathbf{4w^3b + 6w^2b^2 + 4wb^3 + b^4}$ are depicted in the panel. Two arrangements, wwww (w^4) and bbbb (b^4) are nonchimeric. Of the remaining 14 possibilities, only 2 can be unequivocally identified as composed of 4 cells (denoted in red letters). (B) Observed GFP-expressing (g), and GFP-negative (w) ORS sectors in anagen pelage follicles of postnatal day 11 X-inactivation mosaic female mice. Of 130 clones scored, 17 (13.1%) were g/w/g/w.

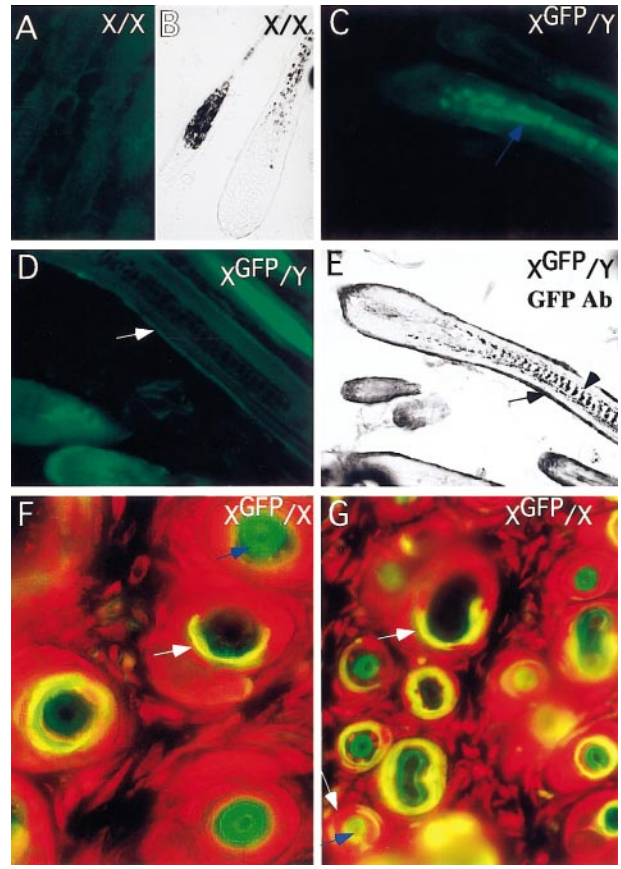

FIG. 7. GFP expression in anagen pelage follicles from postnatal day 11 X-inactivation TgN(GFPX)4Nagy mice. (A–E) Analysis of GFP expression. Wild-type female controls show no GFP fluorescence (A) or immunoreactivity (B) in longitudinal sections of hair follicles. The dark material in (B) is melanin. Pelage follicles from male TgN(GFPX)4Nagy mice shows GFP fluorescence in the medulla (C) and ORS (D). (E) Immunohistochemistry confirms the presence of GFP in the ORS (arrow pointing to black appearing immunoreactive protein). Note that the medulla contains melanin and GFP (e.g., arrowhead). (F, G) Transverse sections of skin containing examples of chimeric follicles. The sections have been counterstained with propidium iodide. GFP fluorescence (green or yellow) is detectable in the medulla (blue arrow), and/or in the ORS (see white arrows pointing to chimeric ORS).

nized, induced anagen. Examples of pelage follicles positioned at the borders between patches of $B6^{ROSA26/+}$ and 129/Sv-derived skin are shown in Figs. 3A–3C. Several of these follicles are chimeric, containing both LacZ+ $B6^{ROSA26/+}$ and LacZ− 129/Sv cells.

A region of dorsal skin with ~130 anagen follicles was serially sectioned to determine the architectural organization of their constituent cell populations. We did not score follicles where chimerism was confined exclusively to the ORS. Unlike the regeneration of the six cell types within the bulb, regeneration of the ORS following depilation or catagen can be fueled either by surviving committed ORS progenitors, by stem cells located in the bulge, or by both (Ghazizadeh and Taichman, 2001; Taylor *et al.*, 2000). This potential for dual contribution would make it exceedingly difficult to interpret the significance of different patterns of ORS chimerism in all but the first embryonic follicles that enter the first catagen at 2 weeks of age (see below).

Forty-five of the 130 follicles exhibited chimerism in more than just the ORS layer. When these were serially sectioned, 40 (89%) contained *sectors* of blue and white cells, while 5 (11%) contained concentric rings composed either of LacZ+ or LacZ− cells. The rare occurrence of concentric rings compared to sectors suggests that the majority of bulb progenitors are not lineage-restricted.

Figure 4 presents 2-D views of two pelage anagen follicles with sectors (Figs. 4A and 4B) and shows that the base of the *bulb* contains a population of Tcf3/4-expressing cells (Fig. 4C; note that stem cells in the *bulge* are known to express these downstream members of the Wnt signaling pathway; DasGupta and Fuchs, 1999; Fuchs *et al.*, 2001; Huelsken *et al.*, 2001; Merrill *et al.*, 2001). The 2-D reconstructions suggest that sectors are composed of either wholly LacZ+ or wholly LacZ− cells and extend upwards from the base of the bulb. Each cohort that forms a sector appears to encompass all six rings of the follicular epithelium: i.e., it extends from the ORS through the innermost ring of the inner root sheath to the medulla. The observation that sectors contain all six epithelial lineages was confirmed in >20 follicles by serial sectioning (e.g., Fig. 4B).

With 2-D reconstructions, irregular borders between cellular cohorts can lead to the impression that there is mixing of cells of opposite genotypes at the boundaries. Therefore, to further verify that these sectors are composed of a homogenous population of cells of a particular genotype, digital images of serial sections were aligned and assembled by using VoxBlast software. This software allowed us to generate 3-D reconstructions of anagen pelage follicles from both types of chimeric mice. The images were rotated, and the sectors inspected from every angle. The results confirm that cells of either genotype contribute to all six epithelial lineages of the hair follicle and that each sector is composed of a wholly LacZ+ or LacZ− cellular cohort (see Fig. 5A, and http://molecool.wustl.edu/kopan.movies.html).

In adult chimeras ($n = 4$) generated by aggregating strain-matched CD1/B6$^{+/+}$ morulae with CD1/B6$^{ROSA26/+}$ morulae, >80% of polyclonal follicles had sectors rather than concentric rings of wholly LacZ+ or LacZ− cells. This result allowed us to conclude that sectoring is not an artifact of a particular method used to generate chimeras, nor a reflection of differences in strain background.

A small population of chimeric anagen follicles containing concentric rings was present in these aggregation chimeras, as in 129/Sv$^{+/+}$ ↔ B6$^{ROSA26/+}$ chimeras. Concentric rings of labeled cells represents the predominant outcome of retroviral transduction of manipulated skin models, while sectors constitute a small minority (Ghazizadeh and Taichman, 2001; Kamimura *et al.*, 1997).

These findings are consistent with the following. In chimeric mice, the majority of follicles contain multipotential progenitors in their bulb (model 3 in Fig. 1 is favored). The appearance of concentric rings in a subpopulation of chimeric follicles would reflect the fraction of follicles supplied by oligo-potential progenitors. In contrast, with manipulated retrovirally infected skin models, either the manipulation per se, or the effect(s) of retroviral infection introduces a bias against the multipotent progenitor populating the bulb. Thus, the majority of the resulting labeled follicles only contain oligo-potential progenitors (i.e., model 2 in Fig. 1 is favored).

The 3-D Reconstruction of Chimeric Anagen Pelage Follicles Provides Estimates of the Number of Multipotent Cells in the Bulb

Three-dimensional reconstruction of serially sectioned chimeric pelage follicles allowed us to address two general questions in the field of mammalian stem biology that have been difficult to answer in most systems. How many active stem cells participate in the generation of a particular structure? In structures that are supplied by more than one oligo- or multipotent stem cell, is the fraction contributed by each stem cell to the structure fixed, or does the activity of a given stem cell fluctuate over time?

Estimating the number of active stem cells per follicle. There are several reasons why the *bulb* of chimeric anagen pelage follicles allows these estimates to be made. First, cell migration within the follicular epithelium is highly organized and very restricted. Differentiating keratinocytes form adherence junctions that restrict their migration to the unkeratinized lower matrix region (Coulombe *et al.*, 1989). Inspection of chimeric follicles disclosed that the borders between cohorts of LacZ+ and LacZ− cells are sharply demarcated, confirming that LacZ+ cells do not freely intermingle with cohorts lacking the marker (see Fig. 4, and Oshima *et al.*, 2001). Second, terminal differentiation of follicular epithelial lineages is not associated with cell loss, unlike the intestinal or corneal epithelium, or the epidermis. Since all cells derived from progenitors are preserved throughout the life of the follicle, the proximal–distal axis of a chimeric follicle provides a historical record of the lineages generated from each of its contributing stem cells (Lin *et al.*, 2000).

To estimate the number of active bulb-associated progenitors, we assumed that they only undergo "quantal divisions": i.e., each divides asymmetrically to generate one

daughter that remains in the stem cell niche, and another that enters the TA pool. In a chimeric follicle, the minimum number of cellular cohorts (sectors) that can be arranged in a circle such that no two identically marked cohorts share a common border is four [e.g., see (v) in Fig. 1C]. If such a follicle contains four active LacZ− stem cells (*w*hite after X-Gal staining), it can be denoted as w^4. Likewise, if a follicle contains two LacZ− and two LacZ+ (*b*lue) stem cells, it can be described as w^2b^2. The probability of occurrence of a particular mixture of four LacZ+ and LacZ− stem cells can be described as $w^4 + \mathbf{4w^3b + 6w^2b^2 + 4wb^3 + b^4}$ (only the boldface probabilities reflect chimeric follicles). Of the 40 chimeric pelage follicles that we analyzed with sectors, the binomial distribution predicts that 17 (43%) will contain 2 active stem cells that produce LacZ− cohorts, and two active stem cells that yield LacZ+ cohorts:

$$\frac{6w^2b^2}{4w^3b + 6w^2b^2 + 4wb^3} = \frac{6}{14} = 43\%. \quad [1]$$

Only one-third (6) of the 17 follicles are predicted to have sectors with neighbors of the opposite marker (w/b/w/b or b/w/b/w in Fig. 6A). This reflects the fact that, in follicles containing four active stem cells, four sectors within a circle can be organized into six possible patterns: **b/w/b/w**, **w/b/w/b**, w/b/b/w, w/w/b/b, b/w/w/b, or b/b/w/w (the bold-faced possibilities represent one-third of these six patterns; all the rest are simply seen as b/w follicles; Fig. 6A).

Only 1 chimeric follicle among the 40 had sectors with neighbors of the opposite marker (Figs. 3D and 5B). Based on the considerations described above, this follicle should have four active multipotent progenitors. The remaining 39 must have fewer than or equal to 4.

The only reliable parameter for judging stem cell number in these types of chimeric systems is the number of cohorts with distinctly marked neighbors per follicle. There are several reasons why we could not refine our estimates further. First, a survey of cross-sections of chimeric follicles does not allow one to distinguish between instances where there are three as opposed to two active stem cells since w/b/W, w/W/b, and w/b all have to be scored as equivalent in a circle. Second, the size of each sector is not a reliable parameter given that there may be variations in the number of TA descendants each stem cell can produce (asymmetric versus symmetric division; variations in mitotic rates of their descendants, etc.). Finally, this analysis provides a conservative upper limit estimate of stem cell number since a follicle containing only two stem cells, whose descendants intermingle, may appear as b/w/b/w.

We also estimated the number of active progenitor cells using a different, noninvasive method that did not involve embryo manipulation or depilation. Follicles were surveyed in the dorsal skin of 11-day-old female mice containing a chicken β-actin/GFP transgene integrated into the X chromosome (TgN(GFPX)4Nagy; Hadjantonakis *et al.*, 1998). Due to the random nature of X inactivation in the embryo (Hadjantonakis *et al.*, 2001), these females contain multiple chimeric follicles.

GFP expression was surveyed by fluorescence microscopy. Analysis of P11 male (nonchimeric) and female (chimeric) mice ($n = 5$) disclosed that GFP expression was confined to the ORS and medulla in >99.9% of the thousands of follicles surveyed—a finding confirmed with immunohistochemistry (Figs. 7A–7E). In rare instances, GFP was also detected in the inner root sheath (data not shown). We did not analyze follicles in $129/Sv^{+/+} \leftrightarrow B6^{ROSA26/+}$ mice where chimerism was confined exclusively to the ORS chimerism since the source of ORS cells in cycling follicles is uncertain (see above). However, the fates of the ORS and inner cell layer lineages separate only after the first hair cell cycle: during the first catagen, the upper part of the ORS survives while the bulb is completely destroyed (Fuchs *et al.*, 2001; Stenn and Paus, 2001). Thus, in postnatal day 11 mice, the lineage relationships of the ORS and the inner layer lineages have not been disturbed. Based on these considerations, we proceeded to analyze the patterns of GFP expression in the ORS/medulla of pelage follicle bulbs, harvested from TgN(GFPX)4Nagy female mice, to estimate the number of active ORS progenitors.

A total of 130 chimeric follicles were scored and placed into 6 categories based on their architecture (Fig. 6B). If there were 5 progenitors per bulb, the binomial distribution predicts that one-third of chimeric follicles would have sectors containing differentially marked GFP-positive (g) or GFP-negative (w) neighbors. This can be expressed as:

$$(w + g)^5 = w^5 + \mathbf{5w^4g + 10w^3g^2 + 10w^2g^3 + 5wg^4} + g^5, \quad [2]$$

where boldface indicates the 30 possible classes of chimeric follicles. Thirty-three percent (10/30) will have distinctly marked neighbors: w/g/w/g/w, g/w/g/w/g, g/w/w/g/w, w/g/g/w/g, g/w/g/w/w, w/g/w/g/g, g/g/w/g/w, w/w/g/w/g, g/w/g/w/w, or w/g/w/g/g. Likewise, the percentage of follicles with sectors flanked by distinctly marked neighbors (w or g) will increase with increases in the number of active stem cells/bulb, or increases in the incidence of mixing of the immediate daughters of two stem cells.

We observed that 17/130 (13.1%) of gw chimeric pelage follicles had distinctly marked neighbors (Figs. 6B and 7F)—consistent with the value predicted for bulbs with 4 active progenitors contributing to the ORS (see Fig. 6A).

Assessing the contributions of bulb stem cells over time. Mouse *whiskers* are specialized hair follicles with unique cycling properties (short catagen leaving the follicle largely intact). A recent elegant study by Oshima and coworkers (2001) demonstrated that in *whiskers* multipotent stem cells originate from the bulge and migrate at a rate of 7–100 μm/day to the bulb. The approach used by Oshima did not allow them to determine whether pelage follicles contain multipotent stem cells. In addition, no information is

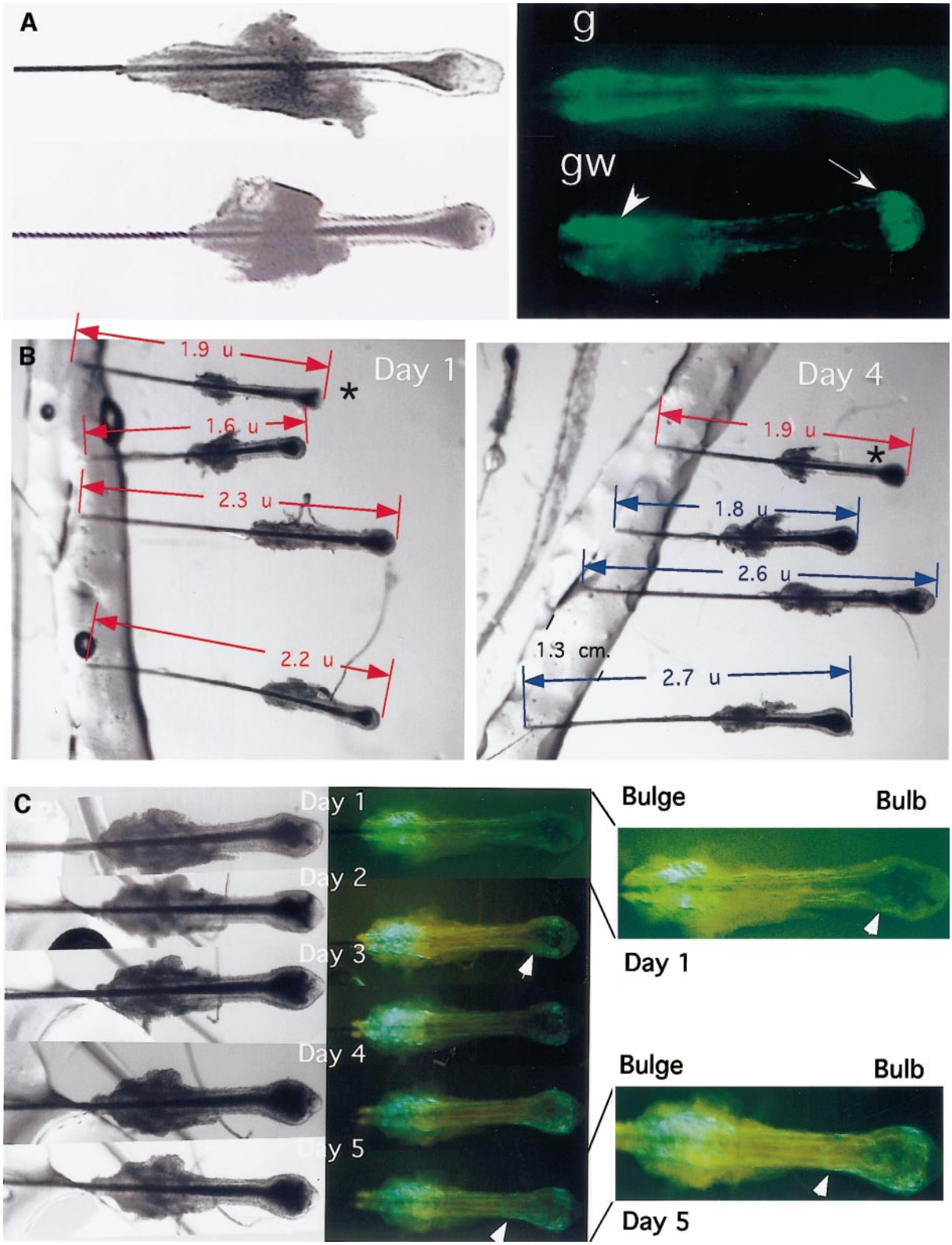

FIG. 8. Analysis of GFP-positive clones in cultured whiskers from TgN(GFPX)4Nagy females. All whiskers in this figure are placed with their distal tip pointing left. (A) Two isolated whiskers after 1 day in culture (bright field image on left, fluorescence on right). One whisker

available from this, or other studies, about whether stem cells migrate from the bulge to the bulb region of pelage follicles during anagen.

If a multipotent bulb stem cell is continuously active throughout anagen, we would predict that that stem cell's progeny would extend in a coherent column along the entire length of the proximal–distal axis of the hair follicle. For 38 of 40 $129/Sv^{+/+} \leftrightarrow B6^{ROSA26/+}$ chimeric pelage follicles, this was the case (e.g., Figs. 5A and 5B). Remarkably, 2/40 follicles contained a homogenous cluster of LacZ− cells at their base, representing all 6 lineages. This "cloistered" cluster did not extend upwards along the full-length of the proximal axis of these follicles (see the 3-D digital reconstruction shown in stereo in Fig. 5C, and the movies at http://molecool.wustl.edu/kopan.movies.html).

It is unlikely that this basal clustering of LacZ− cells is due to incomplete penetration of X-Gal since no partially stained follicles were observed in $B6^{ROSA26/+}$ mice (n = 500 follicles surveyed). One possibility for this finding is that differences in proliferative activity allow the descendents of one multipotent pelage bulb stem cell to overwhelm another. The absence of LacZ− cells in the distal parts of these two follicles suggests that the multipotent stem cell (and its TA daughters) that gives rise to the cloistered clone has a proliferative activity equal to or greater than that in the neighboring stem cell/TA-derived clone. One scenario is that this reflects a previously inactive pelage bulb stem cell becoming active to generate TA daughters in midanagen. Another possibility is that a bulge stem cell was able to enter the bulb during the 7- to 10-day period of pelage follicle regeneration following depilation (i.e., a situation analogous to the whisker).

Cloistered clones are also seen in vibrissal follicles. Although our findings support the notion that the bulb may contain dormant or symmetrically self-renewing multipotential progenitors, we were unable to explore the dynamic behavior of these clones over time by using ROSA26-based chimeras since visualization of LacZ expression requires fixation. We were also unable to examine the behavior of individual GFP-expressing chimeric coat follicles over time due to their small size and the low intensity of their fluorescence when examined by conventional stereomicroscopy.

We were able to gain insights about dynamic clonal behavior by using freshly isolated cultured whisker follicles from 11-day-old female TgN(GFPX)4Nagy pups. Our use of these X-inactivation chimeric whiskers was based on the following considerations. First, at this stage of postnatal development, all whiskers are in their first anagen. Migration of stem cells from the bulge to bulb in whiskers takes a number of weeks (Oshima *et al.*, 2001). Therefore, any changes in the behavior of GFP-positive clones observed during a several-day period of *ex vivo* culture of P11 whiskers should be attributable to changes in the proliferative activities of active stem cells/TA daughters residing in the bulb. Second, we could readily visualize GFP under the stereoscope in whisker follicles (Fig. 8A). Moreover, we were able to identify a high percentage of chimeric whiskers (see follicle marked gw in Fig. 8A).

Individual P11 TgN(GFPX)4Nagy whisker follicles were photographed immediately after dissection, and every 24 h over a 5-day period. Of 17 cultured whiskers, 13 were chimeric (gw). All of the gw whiskers contained cloistered GFP clones in the bulb when isolated (Figs. 8A and 8C). This cloistering was not an artifact of the manipulations required to establish the whiskers in culture: i.e., four whiskers were not chimeric; of these, three were "w" according to the nomenclature given above and one was "g" (the "g" follicle had GFP expression along its entire length; see Fig. 8A).

The length of actively growing cultured chimeric whiskers increases ~10% from day 1 to day 4 of culture (Fig. 8B; note that the control follicle lacking a dermal papilla does not lengthen). There was no evidence of GFP-labeled cells moving toward the bulb from the bulge during the culture period (Fig. 8C).

We found that cloistered GFP clones expanded by 50–100% during this period in four of eight cultured whiskers that were monitored. Movement occurred upward from the bulb (see Fig. 8C, and movie E at http://molecool.wustl.edu/kopan.movies.html). Two of the four whiskers that showed no expansion failed to lengthen during the 4-day culture. The finding that cloistered clones expanded over time at a rate that was faster than the rate of growth of the entire follicle is most consistent with the notion that these bulbs contained stem cell/TA daughters that underwent their first asymmetric division in midanagen.

Following transplantation of hematopoietic stem cells into irradiated mammalian hosts, sequential expansion of clones occurs (Jordan and Lemischka, 1990; Lemischka, 1991). This has led to the suggestion that "dormant" stem cells exist in equilibrium with active stem cell populations

(g) shows GFP fluorescence in all cells (the dark line in the middle of the whisker is due to absorption of the fluorescence signal by melanin). The second whisker is chimeric (gw), with a GFP-positive bulge (arrowhead) and a cloistered GFP clone in the bulb (arrow). (B) Four cultured whiskers, their distal tips embedded in silicone grease. The control whisker lacking the dermal papilla (top, asterisk) did not change in length during the 4-day culture period while the length of the other whiskers increased by ~10% (length is expressed in arbitrary units, u). (C) Cloistered GFP clones in a representative whisker cultured for 5 days. The follicle was embedded in silicone grease and photographed from the same vantage point on successive days by using bright field and UV epi-illumination. The leading edge of GFP positive cells is marked with arrows (higher power images of the whisker on day 1 and 5 are provided on the right). Movement of GFP cells from the bulb towards the bulge can be seen in these static images and in movie E shown at http://molecool.wustl.edu/kopan.movies.html.

(Abkowitz *et al.*, 1995; Jordan and Lemischka, 1990). The cloistered clones we observe in chimeric pelage and vibrissal follicles suggest an analogy between the skin and the reconstituted hematopoietic system. It may be informative to use chimeric mice to examine other slowly renewing epithelia (e.g., the cornea, incisor, nail) to determine whether this is a general epithelial stem cell paradigm.

ACKNOWLEDGMENTS

We are grateful to David Beebe, Rhiner Strorb, Arthur Eisen, Melissa Wong, Emily Garabedian, Jamie Waggoner, Darlene Stewart, and Teresa Tolley for their advice and assistance during the course of these studies. This work was supported by grants from the National Institutes of Health (AR45254 and DK30292). M.H.L. is the recipient of a postdoctoral fellowship from the Dermatology Foundation and Pharmacia–Upjohn.

REFERENCES

Abkowitz, J. L., Persik, M. T., Shelton, G. H., Ott, R. L., Kiklevich, J. V., Catlin, S. N., and Guttorp, P. (1995). Behavior of hematopoietic stem cells in a large animal. *Proc. Natl. Acad. Sci. USA* **92,** 2031–2035.

Cotsarelis, G., Kaur, P., Dhouailly, D., Hengge, U., and Bickenbach, J. (1999). Epithelial stem cells in the skin: Definition, markers, localization and functions. *Exp. Dermatol.* **8,** 80–88.

Coulombe, P. A., Kopan, R., and Fuchs, E. (1989). Expression of keratin K14 in the epidermis and hair follicle: Insights into complex programs of differentiation. *J. Cell Biol.* **109,** 2295–2312.

DasGupta, R., and Fuchs, E. (1999). Multiple roles for activated LEF/TCF transcription complexes during hair follicle development and differentiation. *Development* **126,** 4557–4568.

Fuchs, E., Merrill, B. J., Jamora, C., and DasGupta, R. (2001). At the roots of a never-ending cycle. *Dev. Cell* **1,** 13–25.

Gardner, R. L., and Cockroft, D. L. (1998). Complete dissipation of coherent clonal growth occurs before gastrulation in mouse epiblast. *Development* **125,** 2397–2402.

Ghazizadeh, S., and Taichman, L. (2001). Multiple classes of stem cells in cutaneous epithelium: A lineage analysis of adult mouse skin. *EMBO J.* **20,** 1215–1222.

Hadjantonakis, A. K., Cox, L. L., Tam, P. P., and Nagy, A. (2001). An X-linked GFP transgene reveals unexpected paternal X-chromosome activity in trophoblastic giant cells of the mouse placenta. *Genesis* **29,** 133–140.

Hadjantonakis, A. K., Gertsenstein, M., Ikawa, M., Okabe, M., and Nagy, A. (1998). Non-invasive sexing of preimplantation stage mammalian embryos. *Nat. Genet.* **19,** 220–222.

Hale, P. A., and Ebling, F. J. (1975). The effects of epilation and hormones on the activity of rat hair follicles. *J. Exp. Zool.* **191,** 49–62.

Hardy, M. H. (1992). The secret life of the hair follicle. *Trends Genet.* **8,** 55–61.

Hogan, B., Beddington, R., Costantini, F., and Lacy, E. (1994). "Manipulating the Mouse Embryo: A Laboratory Manual." Cold Spring Harbor Laboratory Press, Plainview, NY.

Huelsken, J., Vogel, R., Erdmann, B., Cotsarelis, G., and Birchmeier, W. (2001). Beta-catenin controls hair follicle morphogenesis and stem cell differentiation in the skin. *Cell* **105,** 533–545.

Johnson, E., and Ebling, F. J. (1964). The effect of plucking hairs during different phases of the follicular cycle. *J. Embryol. Exp. Morphol.* **12,** 465–474.

Jordan, C. T., and Lemischka, I. R. (1990). Clonal and systemic analysis of long-term hematopoiesis in the mouse. *Genes Dev.* **4,** 220–232.

Kamimura, J., Lee, D., Baden, H. P., Brissette, J., and Dotto, G. P. (1997). Primary mouse keratinocyte cultures contain hair follicle progenitor cells with multiple differentiation potential. *J. Invest. Dermatol.* **109,** 534–540.

Kishimoto, J., Burgeson, E. R., and B., M. (2000). Wnt signaling maintains the hair-inducing activity of the dermal papilla. *Genes Dev.* **14,** 1181–1185.

Lemischka, I. R. (1991). Clonal, in vivo behavior of the totipotent hematopoietic stem cell. *Semin. Immunol.* **3,** 349–355.

Lin, M., Leimeister, C., Gessler, M., and Kopan, R. (2000). Activation of the Notch pathway in the hair cortex leads to aberrant differentiation of the adjacent hair-shaft layers. *Development* **127,** 2421–2432.

Merrill, B. J., Gat, U., DasGupta, R., and Fuchs, E. (2001). Tcf3 and Lef1 regulate lineage differentiation of multipotent stem cells in skin. *Genes Dev.* **15,** 1688–1705.

Mintz, B., and Bradl, M. (1991). Mosaic expression of a tyrosinase fusion gene in albino mice yields a heritable striped coat color pattern in transgenic homozygotes. *Proc. Natl. Acad. Sci. USA* **88,** 9643–9647.

Mintz, B., and Silvers, K. (1970). Histocompatibility antigens on melanoblasts and hair follicle cells. *Transplantation* **9,** 497–505.

Oliver, R. F. (1966). Whisker growth after removal of the dermal papilla and lengths of follicle in the hooded rat. *J. Embryol. Exp. Morphol.* **15,** 331–347.

Oshima, H., Rochat, A., Kedzia, C., Kobayashi, K., and Barrandon, Y. (2001). Morphogenesis, and renewal of hair follicles from adult multipotent stem cells. *Cell* **104,** 233–245.

Philpott, M. P., Sanders, D. A., and Kealey, T. (1996). Whole hair follicle culture. *Dermatol. Clin.* **14,** 595–607.

Reynolds, A. J., and Jahoda, C. A. (1991). Hair follicle stem cells? A distinct germinative epidermal cell population is activated in vitro by the presence of hair dermal papilla cells. *J. Cell Sci.* **99,** 373–385.

Reynolds, A. J., and Jahoda, C.A.B. (1996). Hair matrix germinative epidermal cells confer follicle-inducing capabilities on dermal sheath and high passage papilla cells. *Development* **122,** 3085–3094.

Rochat, A., Kobayashi, K., and Barrandon, Y. (1994). Location of stem cells of human hair follicles by clonal analysis. *Cell* **76,** 1063–1073.

Sengel, P. (1976). "Morphogenesis of Skin." Cambridge Univ. Press, Cambridge, U.K.

Stenn, K. S., and Paus, R. (2001). Controls of hair follicle cycling [Review]. *Physiol. Rev.* **81,** 449–494.

Tani, H., Morris, R. J., and Kaur, P. (2000). Enrichment for murine keratinocyte stem cells based on cell surface phenotype. *Proc. Natl. Acad. Sci. USA* **97,** 10960–10965.

Taylor, G., Lehrer, M. S., Jensen, P. J., Sun, T. T., and Lavker, R. M. (2000). Involvement of follicular stem cells in forming not only the follicle but also the epidermis. *Cell* **102,** 451–461.

Topley, G. I., Okuyama, R., Gonzales, J. G., Conti, C., and Dotto,

G. P. (1999). p21(WAF1/Cip1) functions as a suppressor of malignant skin tumor formation and a determinant of keratinocyte stem-cell potential. *Proc. Natl. Acad. Sci. USA* **96,** 9089–9094.

Wong, M. H., Rubinfeld, B., and Gordon, J. I. (1998). Effects of forced expression of an NH2-terminal truncated beta-catenin on mouse intestinal epithelial homeostasis. *J. Cell Biol.* **141,** 765–777.

Zambrowicz, B. P., Imamoto, A., Fiering, S., Herzenberg, L. A., Kerr, W. G., and Soriano, P. (1997). Disruption of overlapping transcripts in the ROSA beta geo 26 gene trap strain leads to widespread expression of beta-galactosidase in mouse embryos and hematopoietic cells. *Proc. Natl. Acad. Sci. USA* **94,** 3789–3794.

Received for publication August 30, 2001
Revised October 18, 2001
Accepted October 18, 2001
Published online January 2, 2002